Influence of zinc coating on nugget development and mechanical properties in dissimilar welded joints DP600 – AISI304 obtained by the RSW process

Alejandro Espinel-Hernández [a], Mario Sánchez-Orozco [b], Angel Sánchez-Roca [b], Lorenzo S. Caputi [c], Louriel Oliveira-Villarinho [d] & Hipólito Carvajal-Fals [e]

[a] National Center of Electromagnetism Applied. University of Oriente. Santiago de Cuba. Cuba. espinel@uo.edu.cu
[b] Materials and Manufacturing Department. Faculty of Mechanical and Industrial Engineering. University of Oriente. Santiago de Cuba. Cuba. mario@uo.edu.cu, sánchez@uo.edu.cu
[c] Surface Nanoscience Group, Department of Physics, University of Calabria. Italy. lorenzo.caputi@fis.unical.it
[d] Faculty of Mechanical Engineering, University of Uberlândia. Uberlândia. Brazil. vilarinho@ufu.br
[e] Federal University of Technology Paraná. Ponta Grossa. Brazil. hcf151@yahoo.es

Abstract
This paper studies the influence of zinc coating of galvanized DP600 steel (DP600G) on nugget development and on the mechanical properties of dissimilar DP600 - AISI304 welded joints obtained by resistance spot welding process (RSW). RSW evaluations consisted of determining, from the dynamic resistance curves, the different stages involved in nugget formation. The experimental results showed that zinc coating on the DP600G steel has a significant influence on the time needed for the start of nugget formation, producing a two times longer delay for non-galvanized steel. Expulsion time was delayed by 1.12 times. The presence of Zn in DP600G/AISI304 welded joints produced smaller nugget diameters as compared to the DP600/AISI304 joints for the same experimental conditions; however, higher peak failure load values were obtained for the former. The causes of this unusual behavior are also analyzed in this paper.

Keywords: resistance spot welding; galvanized steel; dissimilar joints; mechanical properties; nugget development; dynamic resistance.

Influencia del recubrimiento de zinc en la formación del punto y las propiedades mecánicas de la unión disímil DP600 – AISI304 obtenida mediante el proceso RSW

Resumen
Este trabajo investiga la influencia del recubrimiento de zinc del acero DP600 (DP600G) en la formación del punto y las las propiedades mecánicas de las uniones disímiles DP600 - AISI304 obtenidas mediante el proceso de soldadura por resistencia eléctrica por puntos (RSW). El análisis consistió en determinar, a partir de las curvas de resistencia dinámica, las diferentes etapas en la formación del punto. Los resultados experimentales mostraron que el recubrimiento de zinc del acero DP600G influye significativamente en el tiempo necesario para el inicio de la formación del punto, dos veces superior al del acero no galvanizado. El tiempo de la expulsión se retrasó 1,12 veces. La presencia de Zn en las uniones soldadas DP600G/AISI304 produjo diámetros del punto más pequeños en comparación con las uniones DP600/AISI304 para las mismas condiciones experimentales; sin embargo, se obtuvieron valores de carga máxima de fallo más altos para las primeras.

Palabras clave: soldadura por resistencia eléctrica por puntos; aceros galvanizados; soldaduras disímiles; propiedades mecánicas; desarrollo del punto; resistencia dinámica.

1. Introduction

Dual-phase (DP) steel is one of the most widely used Advanced High-Strength Steels (AHSS) used in the automotive industry because of its evident advantages, such as light weight, relatively low cost, safety performance and

good weldability [1]. The Resistance Spot Welding (RSW) behavior of DP steels is well understood through several researches conducted in the past years, some of them focusing on the analysis of RSW welds of DP steels with galvanic coating [2-5].

Ma et al. [2] conducted a microstructural and mechanical characterization of spot-welded hot dipped galvanized DP600 steel. They observed that the hardness in the weld nugget was over two times higher than that in the base metal due to the formation of lath martensite. The crack initiation was observed to occurr basically at the boundary of the weld nugget and at the sheet – sheet interface. Luo et al. [3] developed mathematical models to predict the nugget size and mechanical properties of resistance spot welded joints on galvanized steel sheet. With these prediction results, welding process was also optimized based on the analysis of the effect of process parameters and their interactions on the welding quality. These studies have in common that their authors did not consider the influence of the galvanic coating on the microstructure, mechanical properties or the quality of the welded joints.

Also, Raoelison et al. [4] studied the influence of zinc (Zn) coating on the nugget development during RSW of galvanized steel sheets. They analyzed the enlargement of electro-thermal contact radius due to zinc accumulation during welding and its effect on the formation and growth of the nugget. The authors concluded that at the early stages of welding, zinc coating melts at the interfaces and contact surface increases due to zinc ejection at sheet-sheet and electrode-sheet interfaces, but they do not study the causes of this behavior.

Zn coatings on steel sheets decrease their weldability due to their lower electrical resistance and melting temperature. Zinc coating with low electrical resistance at the faying interface requires that a higher welding current be used to obtain acceptable welded nuggets. Compared to uncoated steels, in galvanized steels, the process of nugget formation changes [5-7].

There is limited literature on how Zn coating affect the RSW process parameters and mechanical properties of dissimilar welded joints of galvanized steels. Khan et al. [8] conducted dissimilar welding experiments between HSLA350 and DP600 steel, both with zinc coating. They evaluated the microstructure and mechanical properties of the welded joints; and concluded that DP600 weld properties played a dominating role in the microstructure and tensile properties of the dissimilar welded joints. The effect of the Zn coating was only assessed in the analysis of the formation of a relative brittle compound at the edges of the weld nugget.

Wei et al. [9] obtained RSW welded joints using similar and dissimilar combinations between galvanized DP1000 steel and TRIP980 cold rolled steel. The authors studied the effect of welding and heat treatment on nugget diameter, hardness distribution and shear strength of the welds. The zinc coat on DP steel surface makes that under the same welding current, the nugget diameter increases in the order of DP/DP, DP/TRIP and TRIP/ TRIP. On the other hand, Jaber et al. [10] analyzed the phase transformations in RSW dissimilar welding between galvanized DP600 steel sheets and AISI430 steel. However, the authors do not evaluate the influence of the Zn coating on the microstructure and

mechanical properties of the welded joints.

Recently, Lin et al. [11] studied the effects of zinc coating thickness on the RSW processing of galvanized mild steel samples. They concluded that when the Zn coating thickness increases, the weldability window becomes narrower. Valaee-Tale et al. [12] proposed an analytical model to predict the critical nugget diameter where expulsion took place; for galvanized and non-galvanized sheets. As a result, they determined that critical nugget diameter for non-galvanized sheets were smaller than that for galvanized ones. What these two papers [11,12] have in common is the study of the influence of zinc coating on galvanized steels in RSW welded joints, however they do not provide further study the causes of these behaviors.

There are few studies on DP600 - AISI304 dissimilar welding. Espinel et al. [13], studied the influence of polarity during RSW of dissimilar DP600 steel and AISI 304 stainless steel. The authors concluded that the positions of the sheets (+)DP600/(-)AISI304 and (+)AISI304/(-)DP600), i.e. polarity, significantly impacted the properties of the joint. Welds made with (+)DP600/(-)AISI304 polarity showed better mechanical properties. Anijdan et al. [14], studied the effect of current density, welding time, electrodes force and holding time on tensile-shear strength of dissimilar joint DP600/AISI304. They reported the optimum conditions for the parameters based on a model obtained by Taguchi method. The authors did not study the effect of Zn coating, usually used on DP600 steel, in dissimilar welding of these materials.

Thus, further research is required on dissimilar welding of galvanized DP600 steels and AISI304 stainless steel using the RSW process. This study is aimed at researching the influence of the zinc coating of galvanized DP600 steel on nugget development and mechanical properties of dissimilar DP600 - AISI304 welded joints using the RSW process.

2. Materials and methods

2.1. Characterization of raw materials

Stainless steel (AISI304) and dual phase steel (DP600) with a thickness of 1.2 mm were used in this experiment. The DP600 steel with a 14 μm galvanic coating per side (DP600G) was used to study the influence of Zn coating on the welding process. The chemical composition and thermophysical properties of the base metals are shown in Table 1 and 2, respectively. The sheets were cut to a dimension of 120 x 38 mm as described in AWS D8.9M:2002 [15].

2.2. Resistance spot welding process (RSW)

A diagram of the experimental setup used is shown in Fig. 1a. RSW welding experiments were performed using a medium frequency direct current machine (MFDC) consisting of a Bosch Rexroth PSG 3100 transformer with a current between 1 and 20 kA, a Bosch PSI6000.100L controller and a pneumatic clamp with an electrode force of 4 kN (Fig. 1b). Experiments were conducted using water-cooled group A, class 1 electrodes Nippert F16CS02, with 3.5 mm of flat tip ends diameter.

Table 1.
Chemical composition of the base metals, wt-%.

Material	C	Mn	Si	S	P	Ni	Cr	Mo	Fe
DP600	0.11	1.6	0.182	-	-	0.027	0.34	0.098	Bal
AISI304	0.08	2.00	1.00	-	-	8	18	-	Bal

Source: own elaboration.

Table 2.
Thermophysical properties of the base metals.

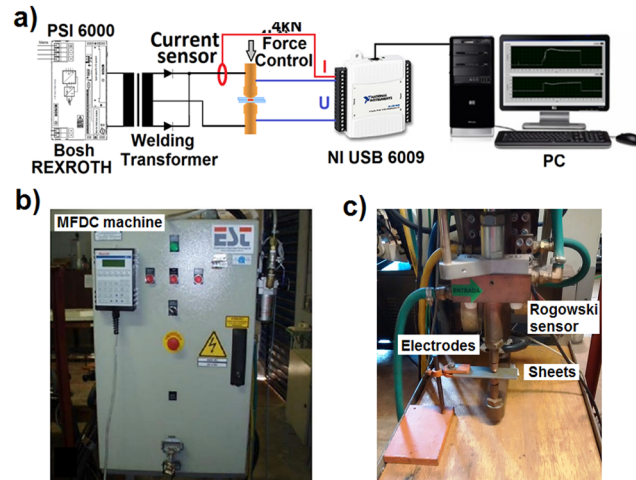| Material	Thermal Conductivity (W/m.°C)	Electrical Resistance (μΩ.m)	Source
DP600	57	0.284	[16]
AISI304	14.6	0.72	[17]

Source: own elaboration.

Figure 1. a) Experimental setup, b) Medium frequency direct current (MFDC) machine and c) Rogowski toroid sensor, electrodes and sheets.
Source: own elaboration.

Figure 2. Diagram of the procedure for sample preparation and macrostructural analysis.
Source: own elaboration.

The experimental setup also consists of a NI USB 6009 data acquisition card to capture in-process current signals measured by a rigid Rogowski toroid sensor (Fig. 1c). An average digital filtering was applied to signal processing. The sampling frequency for the acquisition of the signals was 1.9 kHz.

During the experiment, welding current (I) of 3, 4 and 5 kA, three values of weld time (t): 300, 400 and 500 ms, and the presence or not of galvanic coating on the DP600 steel were used with the aim of evaluating the influence of the Zn coating on the mechanical strength of the welded joint. All welds were randomly performed three times to reduce experimental error. The values of the electrode force, squeeze time, post-weld holding time and up-slope welding current were kept constant.

The selection of the polarity to obtain the dissimilar welded joint was made considering the results of a previous research [13]. This study showed that polarity (+)DP600/(-)AISI304 presented the best mechanical properties and the highest load capacity, 33% higher than those obtained with polarity (-)DP600/(+)AISI304. Welded joints were obtained with the combinations DP600/AISI304 for non-galvanized steel and DP600G/AISI304 for galvanized ones.
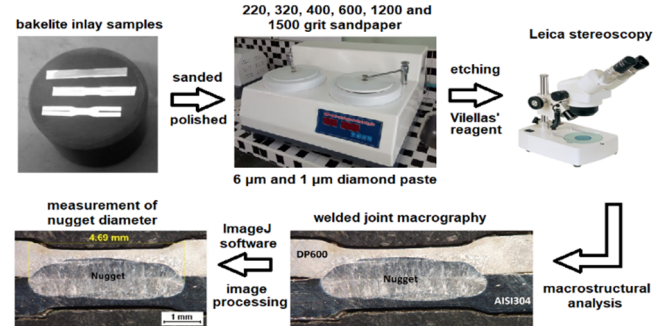
2.3. Characterization of welded joints

To conduct the macrostructural analysis of the welded joints, the samples were transversely sectioned, inserted in bakelite, sanded and polished to a mirror finish. The polished samples were then etched with Vilella's solution during 10 s and rinsed with running water for about 30 s. Macrographs obtained with a Leica stereoscope were used to analyze the influence of the Zn coating on the nugget diameter. For the analysis of the macrographs, digital image processing techniques were applied using the ImageJ 1.48v software. Three measurements of nugget diameter were made per experimental condition. Fig. 2 shows the diagram of the procedure used for sample preparation and macrostructural analysis.

The chemical elements distribution in the cross section of the welded joints were analyzed using Wavelength Dispersive Spectrometry (WDS) by an electron microprobe analyzer (EPMA-Jeol-JXA 8230, 10 kV, 10 nA).

Coach peel tensile tests were performed using a SHIMADZU universal testing machine; model AGX 50 kN, Failure load and displacement values were recorded during the tests. The peak load to failure values extracted from the obtained load–displacement curves is reported in this paper.

A Vickers microhardness tester SHIMADZU HMV-G was used to obtain the hardness profiles covering base metals (BMs), heat-affected zone (HAZ) and fusion zone (FZ) along the sheet-sheet interface; under 100 g indenter load and 15 s dwell time. The hardness indentations were spaced 200 μm apart. Three measurements were conducted for each experimental condition, and average microhardness values were calculated. Both tensile and microhardness tests were carried out in accordance to the AWS/SAE/D8.9:2002 [15].

3. Results and discussion

3.1 Weld joint characterization

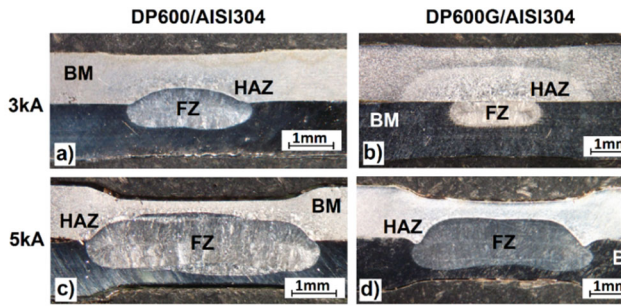The thermophysical properties of materials have a significant influence on the mechanism of nugget formation

Figure 3. Macrographs of cross sections of dissimilar welded joints (t = 500 ms): a) DP600/AISI304 at 3 kA, b) DP600G/AISI304 at 3 kA, c) DP600/AISI304 at 5 kA and d) DP600G/AISI304 at 5 kA.
Source: own elaboration.

Figure 4. Nugget diameter versus weld current for non-galvanized and galvanized DP600/AISI304 joints.
Source: own elaboration.

and its final geometry in dissimilar welding processes [18,19]. As shown in Table 2, AISI304 steel has higher electrical resistivity and lower thermal conductivity than DP600 steel with or without galvanic coating, therefore, a higher heat concentration is generated in the stainless-steel sheet causing the formation of an asymmetric nugget, displaced towards AISI304 side. Fig. 3 shows some typical macrographs of the cross sections of the DP600/AISI304 and DP600G/AISI304 dissimilar welded joints, respectively. In these macrostructures, the three characteristic zones of this type of weld can be identified: the nugget or fusion zone (FZ), the heat affected zone (HAZ) and the base metals (BMs).

The asymmetry of the nugget, characterized by greater penetration on the side of the AISI304 plate, was increased when used the DP600 plate with Zn coating in the joint (Fig. 3b and d). Differences in the thermal conductivity and electrical resistivity of two steel sheets led to an asymmetrical weld nugget in dissimilar metal joints [19]. In Fig. 3b, it can also be observed, that the FZ is completely developed in the AISI304 side, so that an adequate DP600G/AISI304 welded joint is not achieved for the experimental condition of 3 kA and 500 ms. On the other hand, in addition of the nugget asymmetry, the DP600G/AISI304 welded joint obtained for 5 kA and 500 ms suffered plastic deformation at the edges of the nugget, as can be seen in Fig 3d. The causes of this deformation will be analyzed later in this work.

3.2 Influence of Zn coating in nugget diameter

This research corroborates early studies [20-22], that the nugget diameter grows with current intensity due to Joule effect. Fig. 4 shows the nugget diameter versus welding current curves obtained for DP600/AISI304 and DP600G/AISI304 welded joints for the three welding time values analyzed in this paper. The nugget diameter values shown in Fig. 4 refer to three replicates for each experimental condition.

Fig. 4 shows how nugget diameter growths as the welding current increases, with the exception of the welded joints obtained for 5 kA and 500 ms, where a decrease in the nugget diameter was observed for both cases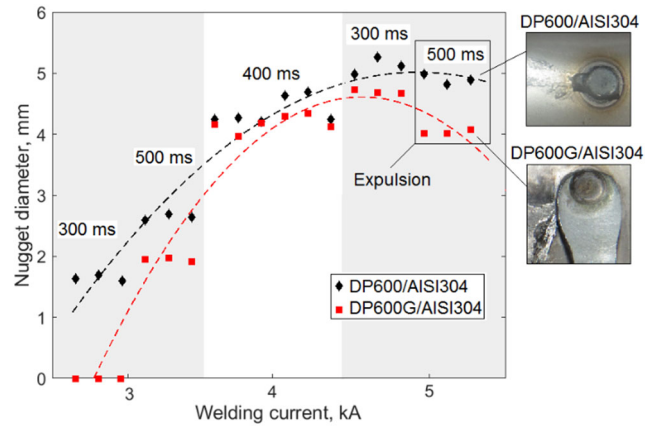. This behavior is due to the occurrence of severe expulsion, which involves the loss of metal from the nugget in the liquid state causing a reduction of the nugget diameter (see images on the right side of Fig 4). As the current increases, the heat input increases by Joule effect, and the volume of molten metal rapidly increases. Under this condition, the external force of the electrode cannot support the internal nugget thermal expansion force, causing the mechanical collapse found around the nugget, which reduces its effective size [23,24].

Figs. 3 and 4, show that the nugget diameter was smaller in DP600 steel welded joints with Zn coating (DP600G/AISI304). By subjecting the galvanized steel to a high rate of heat input, the low melting point of zinc (419 °C) caused the galvanic coating to be displaced from the center of the weld towards the contact area periphery. The resulting unstable geometry of Zn coating leads to a lower and unstable interfacial resistance, so that more energy is required to increase the process temperature as reported by Lin et al [9]. For the parameter set of 3 kA and 300 ms no DP600G/AISI304 welded joints were obtained.

3.3 Effect of Zn coating on dynamic resistance

Fig. 5 shows the dynamic resistance curves where the effect of Zn coating on dynamic resistance can be observed. During the RSW process, dynamic resistance increases until it reaches its maximum value (points t_0 and t_{0G}) and then it drops sharply. This increase in resistance is associated with the heating effect when current begins to flow causing the surface oxide film breakdown before fritting begins, according to Ighodaro et al. [7]. Zn coating on the DP600G steel offers an additional resistance at the sheet/sheet interface (see R_0 values in Table 3), as well as at the electrode/sheet interface [25].
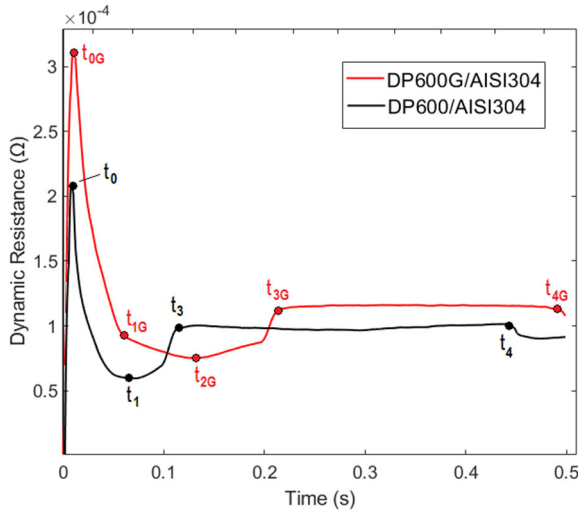
Figure 5. Dynamic resistance curves (Experimental condition: I = 5 kA, t = 500 ms).
Source: own elaboration.

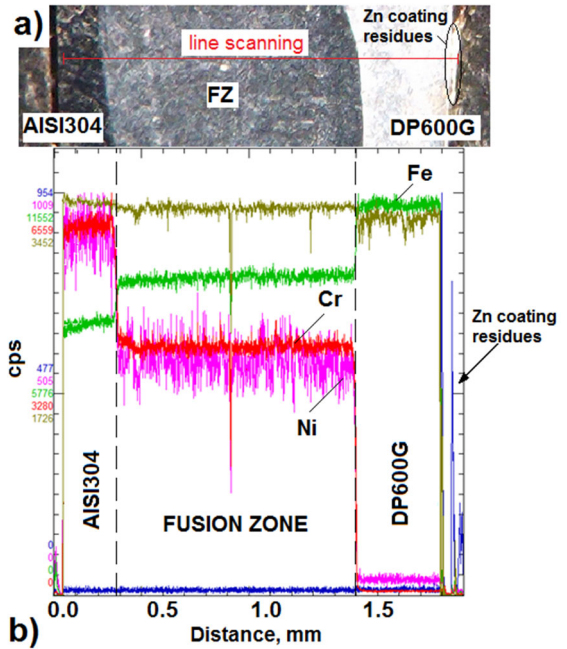
Figure 6. WDS analysis: a) Macrostructure of the cross section and b) Element line scanning results (Condition: I = 5 kA, t = 300 ms).
Source: own elaboration.

Once the breakdown of the surface oxide film and asperities occurs, due to fritting and collapse of some asperities, the contact area increases causing resistance to decrease. Points t_1 and t_{1G}, marks the end of the effect of surface oxide film layer.

Unlike DP600, galvanized DP600 (DP600G) goes through an intermediate stage during the welding process (from point t_{1G} to t_{2G}). During this stage, the energy introduced by the process is used in the heating and softening of the Zn coating for DP600G. Eventually, coating begins to melt and it then spreads and segregates towards the outer edge of the nugget or even vaporizes, increasing the contact surface and leading to a decrease in resistance (R_2 value in Table 3). After the coating is displaced from the sheet/sheet interfaces of DP600G/AISI304 joint, heating is now concentrated on the bulk steel substrate. The resulting sheet/sheet interface resistance and rise in bulk resistance due to an increase in resistivity with temperature cause resistance to increase until it reaches t_{3G} (t_3 for DP600/AISI 304 joints). The nugget starts forming near this point.

In point 3 (t_3 and t_{3G}); melting of the base metals begins. Nugget formation causes the gradual elimination of sheet/sheet interface resistance, hence leading to a reduction in resistance. However, melting causes an increase in resistance of steel due to an increase in resistivity. Due to the opposite directions of these two effects, there may be no obvious change in the dynamic resistance profile. As can be seen in Fig. 5, the resistance value (R_3) at which the fusion of the base metals begins does not differ much between the two cases (see Table 3). Temperature in the welding process starts

to stabilize and nugget growth plays a dominant role until the nugget diameter grows larger than the effective electrode diameter and expulsion occurs (points t_4 and t_{4G}), causing a sharp drop in resistance [12]. Table 3 summarizes the resistance values described above.

As shown in Fig. 5, the presence of this stage (t_{1G} to t_{2G}) during the formation of the DP600G/AISI304 solder joint (not present in the DP600/AISI304 joint) and the influence of the Zn coating itself, results in a delay in the start of nugget formation. The time required in this case is two times longer than that for the DP600/AISI304 joint (experimental condition I = 5 kA, t = 500 ms). Consequently, the average nugget diameter obtained in the DP600G/AISI304 joints is smaller than those observed in the DP600/AISI304 joints (Fig 3).

The delay caused by Zn coating in the beginning of nugget formation also influences the expulsion, which takes longer in the DP600G/AISI304 welded joint (12% higher), compared to the DP600/AISI304 weld, as shown in Fig. 5. Similar dynamic resistance behavior was obtained for all other experimental conditions, except for expulsion that only occurs at I = 5 kA, t = 500 ms.

Fig. 6 shows the chemical element line scanning results of the WDS analysis performed on the cross section of one of the samples of the DP600G/AISI304 welded joint obtained for 5kA and 300 ms.

The WDS analysis showed in Fig. 6 was conducted to corroborate the fact that Zn is segregated towards the outer edge of the nugget, as explained above. The analyzed welded joint consists of Fe, with a higher concentration in the region of the DP600G base metal; Fe, Ni and Cr in the FZ, as a result of the contribution of stainless steel (AISI304) and a third region with a higher presence of Cr and Ni corresponding to AISI304 base metal.

Table 3.
Resistance values during the process stages.

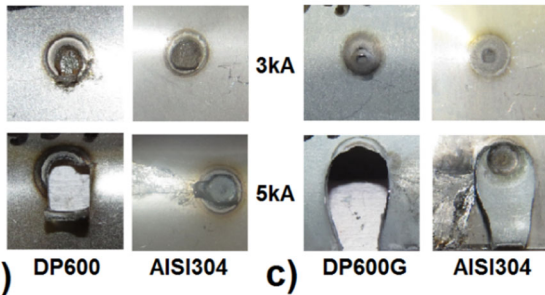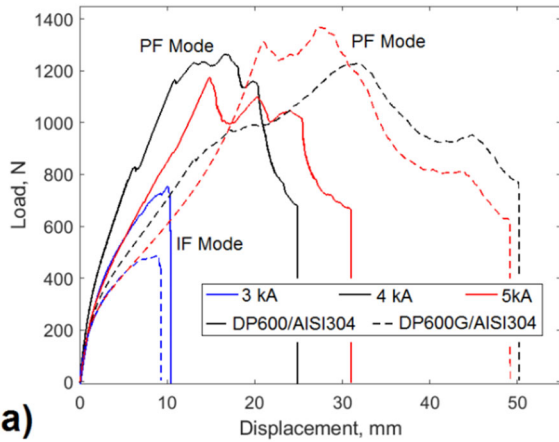|	R_0 x10^{-4} (Ω)	R_1 x10^{-4} (Ω)	R_2 x10^{-4} (Ω)	R_3 x10^{-4} (Ω)	R_4 x10^{-4} (Ω)
DP600/AISI304	2.10	0.59	-	0.99	1.01
DP600G/AISI304	3.11	0.91	0.75	1.13	1.14

Source: own elaboration.

Figure 7. a) Load–displacement curves (t = 500 ms). Failure modes of specimens: b) DP600/AISI304 and c) DP600G/AISI304.
Source: own elaboration.

As shown in Fig. 6, no Zn presence in the nugget of the welded joint was found, which evidences that the galvanic coating was vaporized or segregated in the liquid state towards the edges of the nugget during welding. However, a zinc accumulation is observed at the periphery of the electrode-sheet contact area as a result of the zinc liquid ejection in the early stages of the process.

3.4 Influence of Zn coating on mechanical properties

Fig. 7a shows the load-displacement curves obtained in peel tests for current of 3, 4 and 5 kA and weld time of t = 500 ms. It was found that the highest peak load value (1384.16 N) was reached for the DP600G/AISI304 joint, with a welding current of 5 kA, even though a smaller nugget diameter (4.02 mm) was obtained for this joint. For the conditions shown in Fig. 7a, the largest nugget diameter (4.21 mm) was obtained for DP600/AISI304 joint at current of 4 kA and 500 ms of welding time, for which a peak load value of 1265.14 N was obtained.

Load-displacement curves for all welded joints obtained for a welding current of 3 kA show a characteristic behavior of the interfacial failure (IF) mode (Figs. 7b and c). For 3 kA, the peak value of the curve corresponds to the initiation of the fracture, which rapidly propagates into the nugget causing the load values to fall drastically to zero. For current values of 4 and 5 kA, pull-out failure (PF) modes were observed. The failure modes change from IF to PF with increasing welding current and nugget diameter. Similar results were obtained by Alizadeh-Sh et al. [26]. Figs. 7b and c, show images of the failure modes occurred for the conditions of t = 500 ms and welding current of 3 and 5 kA, respectively. The occurrence of expulsion for the conditions of 5 kA and 500 ms is observed.

For 5 kA experimental conditions, the crack initiated at the edge of the nugget, at which point, the load decreased slightly. The crack then propagated toward the HAZ and entered it at a point where the load greatly decreased. While higher average value of nugget diameter (5.02 mm) were obtained for the DP600/AISI304 welded joints, as compared to the DP600G/AISI304 welded joints, the latter showed higher average maximum failure load (1362.28 N). Therefore, a more detailed analysis of the crack propagation mechanism is needed to understand this unusual behavior. Tables 4 and 5 summarize the average nugget diameter and maximum failure load values obtained for DP600/AISI304 and DP600G/AISI304 welded joints, respectively.

Table 4.
Average nugget diameter and maximum failure load values for DP600/AISI304 welded joints.

t (ms)\I (kA)	Nugget diameter (mm)			Maximum failure load (N)		
	3	4	5	3	4	5
300	1.64	-	5.02	759.73	-	1322.46
400	-	4.38	-	-	1277.52	-
500	2.64	-	4.89	864.74	-	1086.31

Source: own elaboration.

Table 5.
Average nugget diameter and maximum failure load values for DP600/AISI304 welded joints.

t (ms)\I (kA)	Nugget diameter (mm)			Maximum failure load (N)		
	3	4	5	3	4	5
300	0.00	-	4.69	0.00	-	1255.35
400	-	4.18	-	-	1239.12	-
500	1.94	-	4.40	937.7	-	1362.28

Source: own elaboration.

Fig. 8 shows the half of the weld joint macrostructure and the microhardness profiles corresponding to the experimental conditions of 5 kA and 500 ms. In addition, it provides a schematic representation of the indentations made for the microhardness measurement and the assumed crack propagation direction (red line) during the peel tests. Table 6 shows microhardness values obtained in the region of interest.

During the peel test, the stress concentration at the edges of nuggets increases, causing the critical condition of formation and propagation of cracks, leading to fracture. In the DP600/AISI304 joint (Fig. 8a), the crack starts at the sheet-sheet interface and from there it extends directly through the FZ/HAZ boundary to the surface, caused by the hardness gradient, and martensite transformations found in the HAZ region of the DP600 side. Fig. 7b shows the occurrence of this fracture mechanism in the peel test specimen shown.

Table 6.
Microhardness values in the region of interest.

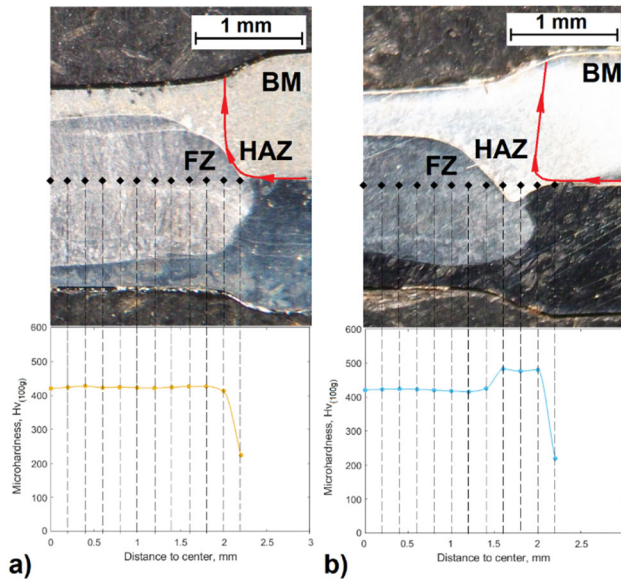| Distance to center (mm)	Microhardness, $Hv_{(100g)}$ (kg/mm^2)											
	0	0.2	0.4	0.6	0.8	1.0	1.2	1.4	1.6	1.8	2.0	2.2
DP600/AISI304	420.8	426.0	428.0	426.6	424.5	422.5	421.7	423.5	426.0	427.8	428.2	222.5
DP600G/AISI304	421.0	422.3	424.0	424.2	420.7	414.2	416.1	433.0	482.4	478.3	480.5	217.0

Source: own elaboration.

Figure 8. Macrostructure and microhardness profile: a) DP600/AISI304, b) DP600G/AISI304.
Source: own elaboration.

When the DP600G was used, at 5 kA and 500 ms, the main deformation occurs at the edge of the nugget in the AISI304 side, as shown in Fig. 8b. The deformation is characterized by the formation of a hook, a region where part of the DP600G sheet penetrates the edge of the nugget formed in the AISI304 stainless steel.

This hook region occurs due to the delay in the formation of the nugget produced by the Zn coating in DP600 steel and also to the differences between the thermophysical properties of the materials of the welded joint. It is clear that AISI304 has greater electrical resistivity and also less heat conduction, which are favorable conditions for the faster growth of the nugget, greater heating in the AISI304 sheet, and therefore greater plasticity of the material. Under these conditions and with constant normal force applied by the electrodes, the DP600 steel, penetrates the AISI304 sheet and deforms the edges of the nugget.

Therefore, the crack that starts between the two sheets in the HAZ-surrounding area due to the stress concentration condition, finds a zone of high hardness caused by the intense plastic deformation in the hook zone in the DP600G side. The result is that the crack propagates through the HAZ/BM boundary in the DP600G steel, based on the failure mode shown in Fig. 7c.

Thus, it can be assumed that the formation of the hook at the edge of the nugget, when using the Zn-coated DP600G steel sheet, is associated with the increased peak load of the welded joint, despite having a smaller nugget diameter in this condition. This means that the Zn coating on DP600G steel, while causing a delay in the formation of the nugget, does not necessarily exert

a negative influence on the mechanical strength of the dissimilar DP600G/AISI304 welded joint. The indentation values for both conditions were less than 25%. There was no significant difference between the indentation values obtained for welded joints with and without Zn coating.

4. Conclusions

On the basis of experimental results and discussion, the major conclusions can be drawn here.

- Zinc coating on the DP600G steel has no a significant influence on the resistance value at which the fusion of the base metals begins. However, it has a significant effect on the time needed for the start of the nugget formation and the occurrence of the expulsion.
- Zn coating produces of two times longer delay on the time needed for the nugget formation in the DP600G/AISI304 welded joints in comparison with DP600/AISI304 joints. Similarly, the expulsion time was delayed by 1.12 times.
- The delay in the nugget formation caused by Zn coating in DP600G/AISI304 dissimilar welded joints, as well as the differences between the thermophysical properties of the two base materials, causes a hook-shaped deformation of the nugget. The increase of the peak load of DP600G/AIS304 welded joints is attributed to the formation of this hook at the edge of the nugget.
- The presence of Zn in DP600G/AISI304 welded joints produced smaller nugget diameters compared to DP600/AISI304 joints for the same experimental conditions, due to the fact that part of the initial energy of the process is used in the heating and melt of Zn coating. However, in the cases where hook formation was observed, higher peak load values were obtained for DP600G/AISI304 joints, despite having a smaller nugget diameter.
- Regardless of the delay in nugget formation caused by the Zn coating present on DP600G steel, DP600G/AISI304 dissimilar welded joints with good mechanical properties can be obtained without the need to add more energy during the process.

References

[1] Pouranvari, M., Marashi, S. and Mousavizadeh, S., Dissimilar resistance spot welding of DP600 dual phase and AISI 1008 low carbon steels: correlation between weld microstructure and mechanical properties,

Ironmaking & Steelmaking, 38(6), pp. 471-480, 2011. https://doi.org/10.1179/1743281211Y.0000000024

[2] Ma, C., Chen, D.L., Bhole, S.D., et al., Microstructure and fracture characteristics of spot-welded DP600 steel, Materials Science and Engineering: A, 485(1–2), pp. 334-346, 2008. http://dx.doi.org/10.1016/j.msea.2007.08.010

[3] Luo, Y., Liu, J., Xu, H., et al., Regression modeling and process analysis of resistance spot welding on galvanized steel sheet, Materials & Design, 30(7), pp. 2547-2555, 2009. http://dx.doi.org/10.1016/j.matdes.2008.09.031

[4] Raoelison, R., Fuentes, A., Rogeon, P., et al., Contact conditions on nugget development during resistance spot welding of Zn coated steel sheets using rounded tip electrodes, Journal of Materials Processing Technology, 212(8), pp. 1663-1669, 2012. http://dx.doi.org/10.1016/j.jmatprotec.2012.03.009

[5] Chan, K., Scotchmer, N., Zhao, J., et al., Weldability improvement using coated electrodes for RSW of HDG steel. SAE Technical Paper; Report No.: 0148-7191, 2006.

[6] Gedeon, S. and Eagar, T., Resistance spot welding of galvanized steel: Part II. Mechanisms of spot weld nugget formation, Metallurgical Transactions B, 17(4), pp. 887-901, 1986.

[7] Ighodaro, O.L.R., Biro, E. and Zhou, Y.N., Study and applications of dynamic resistance profiles during resistance spot welding of coated hot-stamping steels, Metallurgical and Materials Transactions A, 48(2), pp. 745-758. 2017. http://dx.doi.org/10.1016/j.msea.2012.05.085

[8] Khan, M., Bhole, S., Chen, D., et al., Welding behaviour, microstructure and mechanical properties of dissimilar resistance spot welds between galvannealed HSLA350 and DP600 steels, Science and Technology of Welding and Joining, 14(7), pp. 616-625, 2009. https://doi.org/10.1179/136217109X12464549883295

[9] Wei, S.T., Lv, D., Liu, R.D., et al., Similar and dissimilar resistance spot welding of advanced high strength steels: welding and heat treatment procedures, structure and mechanical properties, Science and Technology of Welding and Joining, 19(5), pp. 427-435, 2014. https://doi.org/10.1179/1362171814Y.0000000211

[10] Jaber, H.L., Pouranvari, M., Marashi, S.P.H., et al., Dissimilar spot welding of dual phase steel/ferritic stainless steel: phase transformations, Science and Technology of Welding and Joining, 19(7), pp. 565-571, 2014. https://doi.org/10.1179/1362171814y.0000000226

[11] Lin, H., Hsu, C., Lee, C., et al., Effects of zinc layer thickness on resistance spot welding of galvanized mild steel, Journal of Materials Processing Technology, 251, pp. 205-213, 2018. https://doi.org/10.1016/j.jmatprotec.2017.08.035

[12] Valaee-Tale, M., Sheikhi, M., Mazaheri, Y., et al., Criterion for predicting expulsion in resistance spot welding of steel sheets, Journal of Materials Processing Technology, 275, pp. 116329, 2020. https://doi.org/10.1016/j.jmatprotec.2019.116329

[13] Espinel-Hernández, A., Sánchez-Roca, A., Carvajal-Fals, H., et al., Influence of polarity on mechanical properties of dissimilar resistance spot welds of DP 600/AISI 304 steels, Science and Technology of Welding and Joining. 21(8), pp. 607-613, 2016. http://dx.doi.org/10.1080/13621718.2016.1149913

[14] Anijdan, S.M., Sabzi, M., Ghobeiti-Hasab, M., et al., Optimization of spot welding process parameters in dissimilar joint of dual phase steel DP600 and AISI 304 stainless steel to achieve the highest level of shear-tensile strength, Materials Science and Engineering: A, 726, pp. 120-125, 2018. http://dx.doi.org/10.1016/j.msea.2018.04.072

[15] AWS, A. SAE D8. 9M: Recommended practices for test methods for evaluating the resistance spot welding behavior of automotive sheet steel materials, ISBN: 0-87171-672-0, 2002.

[16] Zhao, D., Wang, Y., Zhang, P., et al., Modeling and experimental research on resistance spot welded joints for dual-phase steel, Materials,12(7), art. 1108, 2019. https://doi.org/10.3390/ma12071108

[17] Chu, T. and Ho, C., Thermal conductivity and electrical resistivity of eight selected AISI stainless steels. Thermal Conductivity 15, pp. 79-104, 1978.

[18] Tsai, C., Papritan, J., Dickinson, D., et al., Modeling of resistance spot weld nugget growth, Welding Journal (USA), 71(2), pp. 47-54, 1992.

[19] Marashi, P., Pouranvari, M., Amirabdollahian, S., et al., Microstructure and failure behavior of dissimilar resistance spot welds between low carbon galvanized and austenitic stainless steels, Materials Science and Engineering: A,480(1), pp. 175-180, 2008. https://doi.org/10.1016/j.msea.2007.07.007

[20] Wan, X., Wang, Y. and Zhang, P., Modelling the effect of welding current on resistance spot welding of DP600 steel, Journal of Materials Processing Technology, 214(11), pp. 2723-2729, 2014. https://doi.org/10.1016/j.jmatprotec.2014.06.009

[21] Jagadeesha, T. and Jothi, T.S., Studies on the influence of process parameters on the AISI 316L resistance spot-welded specimens, The Int J Adv Manuf Technol., 93, pp. 73-88, 2017. https://doi.org/10.1007/s00170-015-7693-y

[22] Safari, M., Mostaan, H., Kh, H.Y., et al., Effects of process parameters on tensile-shear strength and failure mode of resistance spot welds of AISI 201 stainless steel, Int J Adv Manuf Technol., 89, pp. 1853-1863, 2017. https://doi.org/10.1007/s00170-016-9222-z

[23] Ghazanfari, H. and Naderi, M., Expulsion characterization in resistance spot welding by means of a hardness mapping technique, International Journal of Minerals, Metallurgy and Materials, 21(9), pp. 894-897, 2014. https://doi.org/10.1007/s12613-014-0986-6

[24] Ma, C., Bhole, S., Chen, D., et al., Expulsion monitoring in spot welded advanced high strength automotive steels, Science and Technology of Welding and Joining, 11(4), pp. 480-487, 2006. https://doi.org/10.1179/174329306X120895

[25] Saha, D.C., Ji, C.W. and Park, Y.D., Coating behaviour and nugget formation during resistance welding of hot forming steels, Science and Technology of Welding and Joining, 20(8), pp. 708-720, 2015. https://doi.org/10.1179/1362171815Y.0000000054

[26] Alizadeh-Sh, M., Pouranvari, M. and Marashi, S.P.H., Welding metallurgy of stainless steels during resistance spot welding Part II –Heat affected zone and mechanical performance, Science and Technology of Welding and Joining, 20(6), pp. 512-521, 2015. http://dx.doi.org/10.1016/j.matdes.2013.11.022

A. Espinel-Hernández, is a full-time professor in the Department of Informatics at the Faculty of Telecommunications, Informatics and Biomedical Engineering, Universidad de Oriente, Cuba. He earned a BSc. Eng. in Computer Science Engineering in 2010 and a PhD in Technical Sciences in 2020. He currently works on the use of infrared thermography, Deep Learning and Machine Learning techniques for the characterization and optimization of the welding process.
ORCID ID: 0000-0003-4192-363X

M. Sánchez-Orozco, is a full-time professor in Manufacturing and Materials Department at the Faculty of Mechanical and Industrial Engineering, University of Oriente, Cuba. He graduated with a BSc. Eng. in Mechanical Engineering in 1995 and obtained a MSc. in Maintenance Engineering in 1998. He received his PhD in Technical Sciences in 2014 and made his Postdoctoral studies at the Federal University of Uberlandia, Brazil. He was awarded the 2015 Cuba Academy of Sciences Annual Award for his research Influence of microstructure of cemented carbides in damage tolerance induced under service conditions. His current research interests include welding process characterization and surface engineering and coatings.
ORCID ID: 0000-0003-1390-9582

A. Sanchez-Roca, graduated with a BSc. in Automation Engineering in 1995, MSc. in Automation in 2002, and PhD in Technical Sciences in 2006, all from the University of Oriente, Cuba. He is currently a professor in the Department of Manufacturing and Materials at the Faculty of Mechanical and Industrial Engineering at the University of Oriente. Post-doctoral (2011 and 2013) at the Universidade Estadual de Campinas, Brazil. He has experience in automation with applications in manufacturing processes, focusing on the following topics: welding process monitoring, digital signal and image processing, neural networks and acoustic emission. He is currently working on welding processes, with emphasis on process monitoring and control. He has received important awards for his research results.
ORCID ID: 0000-0002-1384-0493

L.S. Caputi, is currently an Associate Professor in the Department of Physics at the University of Calabria, Italy. He started his career as a Surface Scientist investigating the electronic properties of metals surfaces, and is currently head of the Surface Nanoscience Research Group. His current research is basically focused on the synthesis and characterization of carbon-based nanomaterials for the improvement of nanotechnological devices. In particular, exfoliation and oxidation/reduction of natural graphite are applied to obtain graphenic materials.

Moreover, low-cost natural precursors are thermally treated to obtain ultraporous materials for applications in supercapacitors. Prof. Caputi has published 99 papers in peer-reviewed journals.

ORCID ID: 0000-0002-7281-4535

Louriel Oliveira-Vilarinho. Full Professor, researcher and supervisor with a career dedicated to Joining Technologies and Related Processes (welding, additive manufacturing, repair, deposition and cutting) and with history of RD&I granted by private and government funding, within the philosophy of work and coordination of the Laprosolda group - Center for Research and Development of Welding Processes and the EMBRAPII Unit of Metal-Mechanical Technologies. Prof. Vilarinho is author of eleven innovation products and has coordinated and participated in different R.D&I projects granted by governmental agencies (CNPq, Capes, Fapemig and Finep) and companies (Petrobras, White Martins, Daimler-Chrysler, Belgo Bekaert, Usiminas, Air Products, Benteler, among others). He is professor and supervisor of master and doctor candidates in the Post-graduation Program from the School of Mechanical Engineering of Federal University of Uberlandia.

ORCID ID: 0000-0002-3914-156X

Hipolito Domingo Carvajal-Fals. He holds a BS in Mechanical Engineering from the University of Oriente, Cuba. (1986), a master's degree in Mechanical Engineering from the Universidade Estadual de Campinas, Brazil (1995) and a PhD degree in Mechanical Engineering from the Universidade Estadual de Campinas. Brazil (1999). He has broad experience in Mechanical Engineering, focusing on Manufacturing Processes. He is currently a visiting professor at the Federal Technological University of Parana, Parana (Brazil). Prof. Carvajal-Fals conducts research in Welding Processes, Coatings and Surface Engineering. His current projects include Modeling and characterization of friction stir welding processes, Thermal Spray Coating and Surface modification.

ORCID ID: 0000-0001-5061-8763